



Letter

Cite this article: Wolf-Gladrow D, Borrione I, Shirodkar G, Gauns MU, Vadlaman M, Klaas C (2025) In a sea of crumbling icebergs. *Journal of Glaciology* **71**, e76, 1–8. <https://doi.org/10.1017/jog.2025.10060>

Received: 6 December 2024

Revised: 12 May 2025

Accepted: 13 May 2025

Keywords:

iceberg disintegration; ocean-ice interaction; Antarctic Polar Front; marine biogeochemistry; carbon dioxide

Corresponding author: Dieter Wolf-Gladrow;
Email: Dieter.Wolf-Gladrow@awi.de

In a sea of crumbling icebergs

Dieter Wolf-Gladrow¹ , Ines Borrione¹, Gayatri Shirodkar², Mangesh U. Gauns², Murty Vadlaman³ and Christine Klaas¹

¹Marine Biogeosciences, Alfred-Wegener-Institut Helmholtz Zentrum für Polar- und Meeresforschung (AWI), Postfach 12 01 61, Bremerhaven, Germany; ²Chemical Oceanography, CSIR-National Institute of Oceanography (NIO), Goa, India and ³Physical Oceanography Division, CSIR-National Institute of Oceanography, Regional Centre, Visakhapatnam, India

Abstract

In January 2009, on its way from Cape Town to South America (at around 49.5°S and 25°W), the German research vessel *Polarstern* entered a region with a dense cover of icebergs and broken-off chunks of ice up to a few meters in size, largely hidden in a thick fog, a result of the microclimate created by the large agglomeration of icebergs and broken-off glacial ice. Melting of glacial ice led to a cooling (by up to 8°C) and freshening (by up to 2.5 psu) of the surface ocean with perturbations reaching down to about 75 m depth. The observed surface ocean equilibrium fugacity of CO₂, fCO₂, dropped to values that were over 100 μatm lower than atmospheric fCO₂ values. Given the similar concentrations in chlorophyll *a* and the macronutrients nitrate and phosphate inside and outside the perturbed areas, influences of potential iron input from disintegrating icebergs on phytoplankton productivity and fCO₂ can be ruled out. The low fCO₂ values, compared to adjacent regions, can be attributed to thermodynamic effects, i.e. mostly increase of CO₂ solubility with decreasing temperature with a smaller contribution from the dilution due to freshwater inputs. Based on these observations, we consider the potential impact on atmospheric fCO₂ by the release of an armada of icebergs during Heinrich events.

1. Introduction

According to estimates by Davison and others (2023), Antarctic ice shelves exported from 1997 to 2021 on average 2680 ± 580 Gt of freshwater per year to the Southern Ocean, whereby 60% was in the form of solid ice (calving). A spectacular example was iceberg A68A (6000 km² in size) that broke off on 12 July 2017 from the Larsen C ice shelf and drifted for three years toward South Georgia where it stranded on the western shelf of the island in December 2020 (Smith and Bigg, 2023). As for iceberg A68A, an estimated 90% of large icebergs (most of which originate from the ice shelves in the Weddell Sea) transit over the course of several years along the westward flowing coastal current to be steered northward along the Antarctic Peninsula and through the so-called ‘iceberg alley’ into the north and eastward flowing Antarctic Circumpolar Current (ACC). Upon reaching the warmer waters of the Southern ACC and the Polar Front region of the Atlantic sector of the Southern Ocean, large icebergs disintegrate and melt, as evidenced by the fact that they are no longer detectable from satellite imagery (Budge and Long, 2018).

Icebergs can impact biological production by creating natural barriers for marine organisms, releasing trace metals, in particular iron and through the formation of shallow mixed layers due to freshwater input (e.g. Raiswell and others 2008). Alternatively, basal melting could also lead to enhanced (buoyancy driven) surface inputs of nutrients and iron from enriched deep waters (Duprat and others, 2016). The disintegration of icebergs in the Southern Ocean has been observed by whalers and scientists, including Sir Alister Hardy who gave a vivid account of such an event observed whilst on board the RRS *Discovery* in 1926 (Hardy 1967; Supplementary Material (A)). Unfortunately, no investigations were performed at the time. Almost 83 years after the *Discovery* expedition of Sir Alister Hardy the research vessel *Polarstern* encountered similar ‘abnormal local conditions’ in the vicinity of disintegrating icebergs—this time we could carry out an oceanographic survey with diverse and, compared to 1926, improved instrumentation. In the current paper, we report on observations obtained during the *Polarstern* expedition ANT-XXV/3 (PS73). The main goal of this expedition was to carry out the iron fertilization experiment LOHAFEX (Smetacek and Naqvi, 2010; Martin and others, 2013; Schulz and others, 2018). The observations reported and analyzed here were made well before and away from the iron fertilization experiment.

© The Author(s), 2025. Published by Cambridge University Press on behalf of International Glaciological Society. This is an Open Access article, distributed under the terms of the Creative Commons Attribution licence (<http://creativecommons.org/licenses/by/4.0>), which permits unrestricted re-use, distribution and reproduction, provided the original article is properly cited.





Figure 1. Ice broken off from icebergs at 49.55°S, 25.26°W. Photo taken at 21h00 UTC on 18 January 2009 from *Polarstern*. Photo: Dieter Wolf-Gladrow.

2. Materials and methods

Measurements of surface water and atmospheric properties were continually gathered by the ship's thermosalinograph and weather station. Profile measurements (temperature, salinity and pressure) were carried out with a factory-calibrated SBE 911 plus CTD mounted on an SBE32 bottle carousel equipped with 12 L Niskin bottles. Deep (below 800 m) water samples were collected at several stations, for salinity control, using an onboard AUTOSAL (Model No. 8400B, Guideline, Canada). No significant drift in sensor output was observed for the duration of the cruise (Murty and others, 2010). Samples for nutrients and chlorophyll *a* (*Chl a*) profiles were collected with the Niskin bottles at discrete depths. Nutrients were measured with a Skalar segmented flow autoanalyzer using standard procedures (Pratihary and others, 2010). Water samples for *Chl a* analysis were immediately filtered onto GF/F filters and transferred to centrifuge tubes with 10 mL 90% acetone and 1 mL of glass beads, sealed and stored at -20°C for at least 30 min and up to 24 h. *Chl a* was extracted by grinding the filters in a cell mill followed by centrifugation and analysis of the supernatant with a calibrated Turner 10-AU fluorometer following the JGOFS protocol procedure (Knap and others, 1996). Underway $f\text{CO}_2$ measurements during the expedition were carried out using an automated system (General Oceanics, USA): Seawater was drawn continuously from a depth of 11 m and air was pumped from the crow's nest. The mole fraction of CO_2 in the equilibrated air was measured by an infrared analyzer (LiCor) to compute $f\text{CO}_2$ (Dickson *et al.*, 2007). The system was calibrated every 3 hr using calibration gases (CO_2 -in-air mixtures of 310 ppm from MED Gas Agency India and 352.9 and 451.6 ppm CO_2 from Air Liquide).

3. Results

Early morning on 18 January 2009, while steaming in a southwesterly direction, we observed pieces of ice pushed by the wind. The position (near 49°S and 23°W) and advanced season made it very unlikely to encounter sea ice. Hence, the ice must have originated from broken icebergs not yet visible from our position. During the

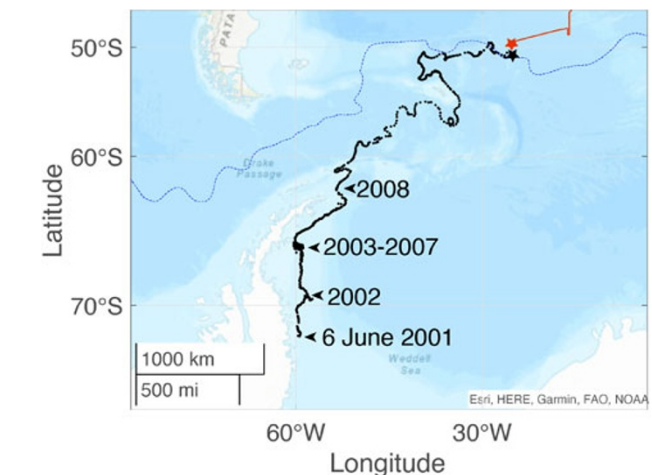


Figure 2. Track of iceberg A43f (black line) determined by satellite scatterometer, from 6 June 2001 to 21 January 2009 (data source: Budge and Long (2018), and <https://www.scp.byu.edu/data/iceberg/>). The black star indicates the last recorded position for A43f on 21 January 2009. The red line shows the track of *Polarstern* until station 102 on 18 January 2009 (indicated by the red star). The dashed blue line marks the (climatological) position of the APF (Orsi and others, 1995). Black arrows show relevant positions and periods of A43f drift trajectory.

following hours, the ice field became denser until almost the whole surface was covered with brash ice and bergy bits up to several meters in size (Fig. 1).

3.1. Origin of the ice field

The iceberg A43 calved off from the Ronne Ice Shelf (Scambos and others, 2005) and later broke into smaller pieces. The track of one of these pieces, namely A43f, was recorded between 6 June 2001 and 21 January 2009 (Fig. 2). A43f was stranded for more than 4 years in the western Weddell Sea (at around 66.6°S, 59.7°W). Thereafter, the iceberg track followed the eastern shelf break of South Georgia and

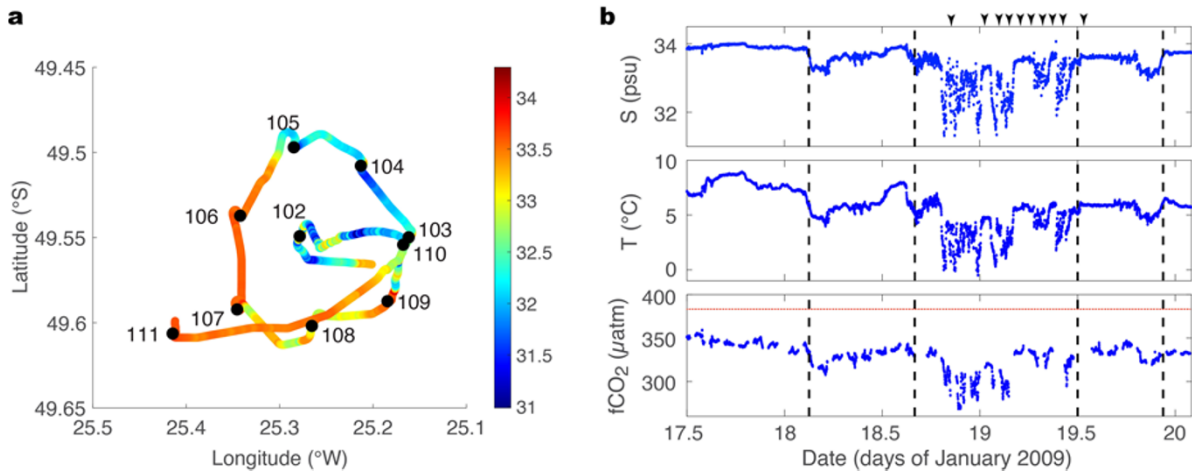


Figure 3. **a**, Location of CTD stations (102–111) between 18 and 19 January 2009 (black circles) and underway salinity (colored dots) from the bow thermosalinograph of *Polarstern*. **b**, Time series (blue lines) of salinity S (upper panel), temperature T (middle panel) and surface ocean $f\text{CO}_2$ (lower panel) from the ship's intake at ~ 11 m depth. The atmospheric $f\text{CO}_2$ is also indicated by the red dotted line in the lower panel. The position of CTD-rossette deployments (stations) is indicated by the black arrows in the upper panel (from left to right stations 102–111). Boundaries of the domains (see text for further details) are indicated by black vertical dotted lines.

into the Georgia Basin where A43f possibly reached the Antarctic Polar Front (APF) for the first time. It then headed eastward and crossed the APF again around December 2008 reaching its northernmost position. Iceberg A43f finally disappeared from the record on 21 January 2009; its last recorded position was 50.77°S , 25.27°W . This likely corresponds to the time and location when A43f finally disintegrated into pieces that were smaller than the scatterometer's iceberg detection limit (resolution 2.2 to 8.9 km/pixel depending on sensor (Budge and Long, 2018)).

The position of the first *Polarstern* station in the area with broken-off glacial ice (Station 102 at 49.55°S , 25.28°W , 18 January 2009, 20h08) was roughly 1° north of the main A43f track. A43f is the only larger iceberg recorded at this time that was close to Station 102. We speculate that the broken ice field encountered by *Polarstern* stem from A43f, broken off probably as A43f reached its northernmost position in the Polar Front region around 5 December 2008, and, while drifting eastward toward our study area, further disintegrated into smaller pieces. According to Orsi and others (1995) the APF marks the northernmost extent of the Winter Water with a temperature minimum of less than 2°C in the upper 200 m. Our hydrographic measurements (CTD profiles down to 500 m, Fig. S1) show that our study area was located close to the APF. Stations 109 ($\theta_{\min} = 1.67^\circ\text{C}$ at $p = 190$ dbar) and 110 ($\theta_{\min} = 1.88^\circ\text{C}$ at $p = 152$ dbar) were south of the APF whereas all other stations (102–108 and 111, temperature minima above 2°C) were in the Polar Front region.

3.2. Cooling, freshening and CO_2

The broken-off glacial ice was melting fast in surface waters at (initially) about 7°C thereby cooling the surface down to slightly below 0°C (minimum -0.67°C ; Fig. 3b). Correspondingly, significant surface water freshening was also observed along the cruise track from the early morning of 18 January 2009 reaching a maximum of more than 2 psu at night from 18 to 19 January 2009. Salinity increased to initial values in the afternoon/evening of 19 January 2009 (Fig. 3b). The underway surface salinity measurements (Fig. 3b) can be used to define domains differing in the intensity of the perturbation:

- (1) an inner core from 18 January 2009 16h to 19 January 2009 12h, in the northeastern quadrant of our study area (Fig. 3a),
- (2) two narrow transitional domains sampled from 18 January 2009 3h to 18 January 2009 16h (first outer core) and from 19 January 2009 12h to 19 January 2009 22h30 (second outer core), respectively,
- (3) two unperturbed areas, south and west of our survey (17 January 2009 12h to 18 January 3h, and 19 January 22h30 to 20 January 2h, respectively).

Before the freshening event, the surface water (based on observations in the unperturbed areas) was already undersaturated in CO_2 (surface ocean fugacity, $f\text{CO}_2$, around $350 \mu\text{atm}$ was smaller than the atmospheric values $f\text{CO}_2^{\text{atm}} = 383 \mu\text{atm}$) most probably due to the seasonal dynamics of biological production, which peaked in mid-November to mid-December, as indicated by the chlorophyll a concentrations estimated from satellite imagery (Fig. S2). Satellite imagery, however, does not indicate substantial differences in chlorophyll a values and its seasonality within the study region, as also indicated by the on-site measurements of chlorophyll a and nutrient concentrations (Fig. S3) in the perturbed (station 102) and unperturbed areas (station 111). A fertilization effect from trace metals and macronutrient input from the icebergs on surface water $f\text{CO}_2$ can, therefore, be rejected based on the abovementioned similarities in satellite-derived chlorophyll a temporal evolution as well as in-situ chlorophyll a and nutrient measurements. In contrast, much lower underway surface $f\text{CO}_2$ values (down to $269 \mu\text{atm}$) were observed in areas with the strongest salinity and temperature perturbations (Fig. 3b). The surface (~ 11 m depth) underway salinity measurements showed the strongest freshening in the northeast quadrant of the circular cruise track (Fig. 3a). The temperature and salinity profiles of station 105 (Fig. S4) in the inner core have been clearly affected by icebergs and the melting of glacial ice.

The disintegration of icebergs followed by fast melting of broken-off small (less than a few meters across) pieces of ice could explain the freshening and cooling of surface waters. The cooling of air above the ocean surface led to an increase in relative humidity (Fig. S5) resulting in a thick fog which made the spatial extent of the ice pieces and icebergs largely invisible. The glacial ice broken

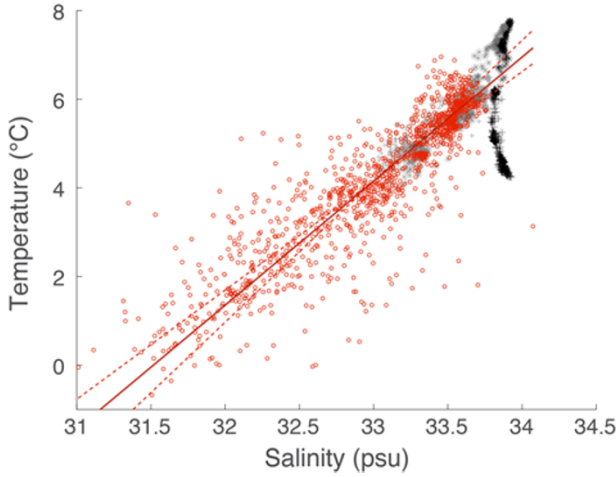


Figure 4. Underway surface ocean salinity versus temperature. Values for the inner core correspond to the red circles. The regression (based only on inner core data) of T on S and S on T are indicated by the dashed red lines. The geometric mean of these two regressions is shown by the red solid line. Values from the transitional domain are indicated by the grey symbols (asterisks: 18 January 3h00 to 16h00; crosses: 19 January 12h00 to 22h30). Values for unperturbed water masses are shown by the black symbols (asterisks: 17 January 12h00 to 18 January 3h00; crosses: 19 January 22h30 to 20 January 12h00).

off from icebergs covered a wide size spectrum with larger pieces of typically a few meters in size (based on visual observation; Fig. 1) and thus melted much faster than the icebergs themselves, thereby cooling and freshening the surface ocean, with temperatures reaching below 0°C . Because the temperature, T , is, in first order, linearly related to heat content (over the relevant S and T ranges, the heat capacity of seawater, c_p , varies by less than 1%), S and T should be linearly related to each other, i.e.

$$T(S) = \beta S + \beta_0. \quad (1)$$

The intercept, β_0 , and slope, β , have been estimated from our underway data through regression of T on S and by regression of S on T (Fig. 4: red dashed lines). The regressions yield: $\beta_{0,T \text{ on } S} = -77.1 \pm 1.3^\circ\text{C}$, $\beta_{T \text{ on } S} = 2.46 \pm 0.04^\circ\text{C psu}^{-1}$, and $\beta_{0,S \text{ on } T} = -100.7 \pm 1.5^\circ\text{C}$, $\beta_{S \text{ on } T} = 3.18 \pm 0.04^\circ\text{C psu}^{-1}$. The slope of the ‘geometric line’ (Draper and Smith, 1998) crossing the centroid of the data is calculated as the geometric mean of the two regression lines, yielding $\beta_{0,\text{geom.}} = -88.2 \pm 1.4^\circ\text{C}$; $\beta_{\text{geom.}} = 2.80 \pm 0.04^\circ\text{C psu}^{-1}$, (Fig. 4, red solid line); the uncertainty of the geometric slope was estimated according to expressions given by Isobe and others (1990) and Babu and Feigelson (1992).

3.3. A model for the relationship between T and S

The slope, β , and intercept, β_0 can also be estimated based on the mass, salt and energy balances yielding values that vary slightly depending on the assumption made about the iceberg core temperature (-20°C or 0°C). Observations of iceberg core temperatures in the North Atlantic range between -20°C and -15°C (Diemand, 1984) with the outer few meters of icebergs affected by heat exchange with the surroundings (Løset, 1993). To the best of our knowledge, no measurements of core temperatures of icebergs in the Southern Ocean have been carried out so far; however, temperatures are expected to be close to values before calving (around -20°C , Hartmut Hellmer, personal communication, 2011). Low ($< 0^\circ\text{C}$) ice temperatures are supported by the low water ($< 0^\circ\text{C}$)

temperatures found during our study (Fig. 4). In our theoretical considerations below we therefore assume two different iceberg core temperatures representing the likely lower and upper temperature boundaries for the icebergs found in our study area, namely -20°C for no warming during its long journey from calving to disintegration and 0°C for warming already to the melting point. Heating pure ice from -20°C to the melting temperature at 0°C requires 42.2 kJ kg^{-1} ($\Delta T = 20^\circ\text{C}$ times the heat capacity of pure ice, $c_{p,\text{ice}} = 2.11 \text{ kJ kg}^{-1}\text{C}^{-1}$, Petrich and Eicken 2010), corresponding to 13% of the latent heat of fusion, L_m , required for the melting of ice ($L_m = 333.4 \text{ kJ kg}^{-1}$, Petrich and Eicken 2010).

The impact of ice melting on surrounding water temperature and salinity can be estimated as follows. The internal energy of seawater, E (J kg^{-1}) is given by

$$E = c_{p,\text{sw}} T_{\text{sw}} + E_0 \quad (2)$$

where T_{sw} ($^\circ\text{C}$) is the temperature of seawater, $c_{p,\text{sw}}$ ($\text{J kg}^{-1}\text{C}^{-1}$) is the specific heat (or heat capacity) of seawater at constant pressure ($3.985 \text{ kJ kg}^{-1}\text{C}^{-1}$ at $S = 35$, $T = 7^\circ\text{C}$, surface pressure), and E_0 is a constant that will drop out in the energy balance below (Eq. 5). The heat capacity of water, c_p , varies slightly with temperature, salinity and pressure (Gill, 1982). These small variations will be neglected here. When $x \text{ kg}$ of ice melt in $y \text{ kg}$ of seawater, mass, salt and energy balances read:

$$x + y = z \quad (3)$$

$$y S_i = z S_f \quad (4)$$

$$y c_{p,\text{sw}} (T_{\text{sw},i} - T_{\text{sw},f}) = x L_m - x c_{p,\text{ice}} T_{\text{ice},i} + x c_{p,\text{sw}} T_{\text{sw},f} \quad (5)$$

where S_i is the initial water salinity, S_f is the final (after dilution) salinity, $T_{\text{sw},i}$ ($^\circ\text{C}$) is the initial water temperature, $T_{\text{ice},i}$ ($^\circ\text{C}$) is the internal ice core temperature, and $T_{\text{sw},f}$ ($^\circ\text{C}$) is the final (after cooling) water temperature. In the balances (Eqs. 3-5) we neglect the exchange of water (evaporation, precipitation) or heat with the atmosphere. This should be a valid assumption on short time scales, despite the fact that some heat exchange with the atmosphere took place indicated by the cooling of the atmosphere leading to the formation of thick fog. For known initial salinity, S_i , and observed final salinity, S_f , one can calculate the glacial freshwater input:

$$x = z - y = z - z \frac{S_f}{S_i} = z \left(1 - \frac{S_f}{S_i} \right) \quad (6)$$

Inserting this relationship into the energy balance (Eq. 5) leads to

$$z \frac{S_f}{S_i} c_{p,\text{sw}} (T_{\text{sw},i} - T_{\text{sw},f}) = z \left(1 - \frac{S_f}{S_i} \right) (L_m - c_{p,\text{ice}} T_{\text{ice},i} + c_{p,\text{sw}} T_{\text{sw},f}) \quad (7)$$

or (z drops out and multiplication by S_i)

$$S_f c_{p,\text{sw}} (T_{\text{sw},i} - T_{\text{sw},f}) = (S_i - S_f) (L_m - c_{p,\text{ice}} T_{\text{ice},i} + c_{p,\text{sw}} T_{\text{sw},f}) \quad (8)$$

which is readily solved for $T_{\text{sw},f}$

$$T_{\text{sw},f} = \beta S_f + \beta_0 \quad (9)$$

with

$$\beta = \frac{L_m + c_{p,\text{sw}} T_{\text{sw},i} - c_{p,\text{ice}} T_{\text{ice},i}}{S_i c_{p,\text{sw}}} \quad (10)$$

and

$$\beta_0 = -\frac{L_m - c_{p,ice}T_{ice,i}}{c_{p,sw}} \quad (11)$$

The slope β (Eq. 10) has been derived as an approximation by Gade (1979) and is usually called the ‘Gade slope’ (e.g. Straneo and Cenedese, 2015). For $S_i = 33.88$, $T_{sw,i} = 7.10^\circ\text{C}$ one obtains $\beta_{0^\circ\text{C}} = 2.68^\circ\text{C psu}^{-1}$ and $\beta_{0,0^\circ\text{C}} = -83.7^\circ\text{C}$ assuming $T_{ice,i} = 0^\circ\text{C}$ (ice close at the melting point, from the outer layers of the iceberg) or $\beta_{-20^\circ\text{C}} = 2.99^\circ\text{C psu}^{-1}$ and $\beta_{0,-20^\circ\text{C}} = -94.3^\circ\text{C}$ assuming $T_{ice,i} = -20^\circ\text{C}$. Our geometric regression parameters are within the range of model-based estimates for β and β_0 for initial ice temperatures of -20°C and 0°C :

$$\begin{aligned} \beta_{0^\circ\text{C}} = 2.68^\circ\text{C psu}^{-1} &< \beta_{geom.} = 2.80^\circ\text{C psu}^{-1} \\ < \beta_{-20^\circ\text{C}} = 2.99^\circ\text{C psu}^{-1} &< \beta_{0,geom.} = -88.2^\circ\text{C} \\ \beta_{0,-20^\circ\text{C}} = -94.3^\circ\text{C} &< \\ < \beta_{0,0^\circ\text{C}} = -83.7^\circ\text{C}. & \end{aligned}$$

3.4. Impact of dilution and cooling on $f\text{CO}_2$

In the southern hemisphere, $f\text{CO}_2^{\text{atm}}$ does not vary much on sub-seasonal times scales (and is primarily influenced by air pressure variations). The solubility of CO_2 in seawater is primarily a function of water temperature, with cooling leading to large decreases of equilibrium fugacity of CO_2 in seawater. In equilibrium, the fugacity of CO_2 is related to the concentration of CO_2 in seawater, $[\text{CO}_2]$, by Henry’s law (e.g. Zeebe and Wolf-Gladrow 2001)

$$[\text{CO}_2] = K_0(T, S) \cdot f_{\text{CO}_2} \quad (12)$$

where $K_0(T, S)$ is Henry’s constant for CO_2 . Cooling leads to large decrease of f_{CO_2} because $K_0(T, S)$ shows strong variation with temperature (Weiss, 1974). In order to calculate the variations of f_{CO_2} , we first estimate $[\text{CO}_2]$ from the following initial conditions: $S_i = 33.88$ psu, $T_{sw,i} = 7.10^\circ\text{C}$, $f_{\text{CO}_2,i} = 351 \mu\text{atm}$, $\text{TA}_i = 2272 \mu\text{mol kg}^{-1}$ (TA = total alkalinity; GLODAPv2, surface value at 49.5°S , 24.5°W) yielding $[\text{CO}_2] = 17.1 \mu\text{mol kg}^{-1}$ and $\text{DIC} = 2094 \mu\text{mol kg}^{-1}$ (DIC = dissolved inorganic carbon). Before estimating the change in f_{CO_2} by the combined effect of cooling and dilution, we calculate the fugacity changes (sensitivities) for cooling and dilution separately:

$$\left(\frac{\partial f_{\text{CO}_2}}{\partial T}\right)_{S=\text{const}} = 15.1 \mu\text{atm}^\circ\text{C}^{-1} \quad (13)$$

and

$$\left(\frac{\partial f_{\text{CO}_2}}{\partial S}\right)_{T=\text{const}} = 15.5 \mu\text{atm psu}^{-1} \quad (14)$$

For the combined effect of cooling and dilution one obtains

$$\left(\frac{\partial f_{\text{CO}_2}}{\partial T}\right)_{\Delta T=\beta\Delta S} = 19.5 \mu\text{atm}^\circ\text{C}^{-1} \quad (15)$$

This sensitivity ($19.5 \mu\text{atm}^\circ\text{C}^{-1}$) is large enough to explain the large observed perturbations in f_{CO_2} (Fig. 3b, bottom panel) in combination with observed perturbation of T and S . All calculations were done using the CO2sys.m Version v3.1.1, 2021, <https://github.com/jonathansharp/CO2-System-Extd>.

3.5. Impact of disintegrating icebergs during Heinrich events

The only documented ice-sheet collapse in the Earth’s history is the release of a large armada of icebergs from the Laurentide ice sheet

at the Hudson Bay, identified as the cause of the Heinrich events (Heinrich, 1988) H1, H2, H4, H5 (Hemming, 2004). The amount of freshwater input from icebergs has been estimated to be 0.29 ± 0.05 Sverdrup (1 Sverdrup = $10^6 \text{ m}^3 \text{ s}^{-1}$) lasting for 250 ± 150 yr (Roche and others, 2004) or about $2.3 \cdot 10^{18}$ kg in total. Based on the observations from our study, we calculate a rough estimate for the potential CO_2 uptake by the cooling and dilution of seawater and the re-equilibration of ocean $f\text{CO}_2$ with the glacial atmospheric $f\text{CO}_2$. For the sake of simplicity, we neglect re-equilibration of temperature, the fate of CO_2 taken up by the ocean surface layer and feedback as, for example, the atmospheric response to surface ocean cooling (Lee and others 2011 and Fig. S5).

Solving the energy balance (Supplementary Material (B)) we determine that cooling 100 kg of seawater by 1°C requires 1 kg of ice (assuming an internal iceberg temperature of -20°C , Diemand 1984). Assuming that seawater with a typical total alkalinity (TA) of $2300 \mu\text{mol kg}^{-1}$, $T = 6^\circ\text{C}$, $S = 35$, is initially in equilibrium with an atmosphere of $200 \mu\text{atm}$ CO_2 fugacity requires $\text{DIC} = 2021.5 \mu\text{mol kg}^{-1}$. A cooling by 1°C leads to a decrease of $f\text{CO}_2^{\text{oc}}$ to $191.2 \mu\text{atm}$. In order to re-equilibrate with the atmospheric $f\text{CO}_2$ of $200 \mu\text{atm}$, CO_2 has to be taken up from the atmosphere until DIC reaches $2030.3 \mu\text{mol kg}^{-1}$. For the total input of glacial ice ($2.3 \cdot 10^{18}$ kg) and the cooling capacity of glacial ice one obtains an uptake of 24 Pg C.

The addition of freshwater from melting glacial ice leads to freshening and dilution of TA and DIC. Dilution by 1% results in $S = 34.65$, $\text{TA} = 2277 \mu\text{mol kg}^{-1}$, $\text{DIC} = 2001.3 \mu\text{mol kg}^{-1}$ and thus $f\text{CO}_2^{\text{oc}} = 196.9 \mu\text{atm}$. Re-equilibration with the atmospheric $f\text{CO}_2$ of $200 \mu\text{atm}$ requires the uptake of CO_2 from the atmosphere until $\text{DIC} = 2004.4 \mu\text{mol kg}^{-1}$ is reached. For the total input of glacial ice ($2.3 \cdot 10^{18}$ kg) one obtains an additional uptake of 8 Pg C.

An uptake of 8 Pg C (or even 32 Pg C) over a time span of 250 yr would be hardly recognizable in ice core records of atmospheric CO_2 . However, the impact of icebergs on the hydrography (stratification, mixing; e.g. Helly and others 2011; Stephenson and others 2011) can have a significant effect on nutrient supply (via deep mixing) and primary production.

4. Discussion

The cooling and freshening of surface waters by melting of glacial ice has been extensively investigated (e.g. Helly and others (2011); Stephenson and others (2011) and Meire and others (2015), to name a few). However, our study is the first to document, by in-situ observations of hydrography and chemical parameters, impacts by fast disintegration of icebergs in the Antarctic Polar Front region. The large perturbations in temperature and salinity are due to the fact that the disintegration of icebergs took place in relatively warm waters ($> 7^\circ\text{C}$) near the Antarctic Polar Front likely leading to a very fast generation of broken-off small (< 10 m, Fig. 1) pieces of glacial ice that melt much faster than the icebergs. We not only report a unique set of temperature-salinity data but also compare the estimated covariation of salinity and temperature ($T-S$ curve, slope β , Fig. 4, Eq. 1) with theoretical values based on the balance (conservation) of mass, salt and energy.

The investigation of melting of ice in seawater has a long history going back to experimental work by Pettersson (1878); (1900); (1904); (1907) and Nansen (1906); (1912). The interpretation of laboratory experiments was complicated by double-diffusion, by fast exchange of heat before the release of meltwater leading to a decrease in salinity, and by the onset of convection, depending on various experimental conditions (Gade, 1979). The $T-S$ slope (β)

due to ice melting was calculated already by Matthews and Quinlan (1975) who obtained a value of $2.56^{\circ}\text{C psu}^{-1}$. Their approach was criticized by Gade (1979) who pointed out that Matthews and Quinlan (1975) had neglected the heat required to warm the ice to its melting temperature and the heating of the meltwater to the surrounding temperature. Based on an internal ice temperature of -10°C and $T_{\text{sw},i} = 3.3^{\circ}\text{C}$, $S_i = 31$ psu, Gade (1979) obtained a slope of $2.94^{\circ}\text{C psu}^{-1}$. These theoretical slope values depend not only on ice and water properties (L_m , $c_{p,\text{ice}}$, $c_{p,\text{sw}}$) but also on initial conditions ($T_{\text{ice},i}$, $T_{\text{sw},i}$, S_i ; Eq. 10) and cannot be compared to each other for different initial conditions. The slope value estimated from our data, $2.80^{\circ}\text{C psu}^{-1}$, would correspond to an internal ice temperature of about -8°C .

Freshening and cooling by glacial ice melt have opposite effects on the density of seawater. For the observed changes in T and S in our study area, the freshening effect on density is dominant. Thus, in general cooling and freshening by disintegrating icebergs at the APF reduce the density of surface waters having the potential to impact circulation and the overall CO_2 sink of the Southern Ocean in the long run. This is compounded by the impact of SST on local atmospheric conditions (Fig. S5), in particular, the thick fog covering the area.

The area with reduced sea surface temperature (SST) included in our survey extended between about 25.16°W and 25.29°W and between 49.485°S to 49.564°S covering an area of about 100 km^2 (Fig. S6) and is thereby larger than pixel sizes for SST determination from satellites (e.g. Merchant and others 2019, give 1 to 45 km^2). We could, however, not see the SST signal from satellite imagery. Hence, the impact of collapsing large icebergs in the area might be overlooked when using satellite products.

Given the logistical constraints, observations on the impact of iceberg disintegration and melting are sparse. In a study of the drifting iceberg C18a in the Weddell Sea (note that C18 originated in the Ross Sea), Helly and others (2011) also recorded very low values of pCO_2 —down to almost $280\text{ }\mu\text{atm}$ (Fig. 2E in Helly and others 2011). Helly and others (2011) and Vernet and others 2011 discuss in detail the factors that could have potentially explained both the $\text{Chl } a$ temporal dynamics and pCO_2 values observed; the authors attribute the pCO_2 decrease to biological production. Meire and others (2015), in a study of the marine carbonate system in the Godthåbsfjord and in coastal water adjacent to the Greenland Ice Sheet, also observed low pCO_2 associated with glacial water input. They attributed the low pCO_2 largely ($> 2/3$) to primary production and $1/3$ to the input of glacial meltwater based on a laboratory end-member measurement for freshwater (FW) derived from thawing glacial ice of ($S_{\text{FW}} = 0$), $\text{DIC}_{\text{FW}} = 80 \pm 17\text{ }\mu\text{mol kg}^{-1}$ and $\text{TA}_{\text{FW}} = 50 \pm 20\text{ }\mu\text{mol kg}^{-1}$. The smaller TA than DIC for their FW values is not explained by the authors, suggesting that their estimates of the impact of glacial water on surface ocean pCO_2 might be biased. Further, although the carbonate system was over-determined by measuring DIC, TA and pCO_2 (Meire and others, 2015), no consistency analysis is reported in the study. Henson and others (2023) measured DIC, TA, T and S in various Greenland fjords, but did not discuss pCO_2 variations. Tarling and others 2024 studied the collapse of iceberg A-68A, however, they did not report any measurements of carbonate system parameters. In contrast to these previous investigations, we find that, in our study area, the impact of cooling and freshening by the melting glacial ice is large enough to explain the drop in fCO_2 by up to $80\text{ }\mu\text{atm}$ (Fig. 3b). The main difference in the direct impact of glacial ice input between our and the abovementioned studies is the size of the temperature perturbation which is much larger for the rapid

iceberg disintegration in the relatively warm waters at the Antarctic Polar Front. Further, the concurrence of our study with the disintegration of iceberg A43f, which was likely still ongoing, given the large amount of floating brash ice (Fig. 1), as well as the nutrient and $\text{Chl } a$ values found on site, suggest no significant impact of changes in biological activity yet.

The combined oceanic uptake of 32 PgC during Heinrich events is possibly an overestimate as heat exchange with the atmosphere and impacts on mixed layer dynamics and circulation are not considered. Our findings show that iceberg disintegrations also affect atmospheric conditions (Fig. S5), hence, estimating the impact of Heinrich events on carbon cycling warrants further investigations using Earth System Models.

Finally, simulations of iceberg trajectories (Merino and others, 2016; Rackow and others, 2017) included various mass loss processes (erosion by surface waves, basal melting), however, the breakup or collapse into smaller icebergs and fast-melting glacial ice with a broad range in sizes have not been taken into account. The neglect of fast disintegration processes might explain the overestimation of trajectory lengths in these simulations and has been addressed by more recent work (England and others, 2020). Based on our findings, the perturbation caused by disintegrating icebergs is large enough in terms of area (order of 100 km^2 or more) and temperature (decrease by several degrees Celsius) to be detected by satellite and allowing to follow the evolution of the perturbed water mass. The horizontal density contrasts between the lighter (because fresher) water mass and the surrounding waters is up to 1 kg m^{-3} over small horizontal length scale of the order of one kilometer or less. This strong horizontal density gradient should drive a cyclonic flow around the center of the perturbed area. One could speculate that this mechanism might lead to the formation of small eddies although strong jet streams in the front region might prevent the buildup of such structures or quickly destroy them. If fast iceberg disintegrations are indeed triggered by encounters with the APF one can expect a freshwater input in the frontal zone that is larger than in adjacent waters. This freshwater input may temporally impact the dynamics and structure of the frontal region.

5. Conclusions

While steaming to the selected location for the iron fertilization experiment (LOHAFEX), we were lucky enough to encounter a field of melting glacial ice, providing us with a unique opportunity to study the ‘abnormal local conditions’ (Hardy, 1967) generated by the disintegration of icebergs. Our study shows that the fast disintegration of icebergs when reaching warmer conditions can lead to substantial local cooling and freshening of the ocean with considerable perturbations down to at least 75 m depth. The observed correlation between variations in temperature and salinity can be explained by a simple model based on the conservation of mass, salt and energy. As a consequence of the cooling, with additional smaller effects due to freshening, fCO_2 in the study area decreased from about $350\text{ }\mu\text{atm}$ down to $269\text{ }\mu\text{atm}$, i.e. causing a very strong undersaturation of CO_2 with respect to the atmosphere. This undersaturation would lead to enhanced uptake of CO_2 by the ocean. The atmospheric micro-climate generated by disintegrating icebergs might be also worth further investigation (Fig. S5). The fast disintegration of A43f was most probably triggered by temperature changes while crossing the Antarctic Polar Front (APF). If such processes are typical for icebergs in the Atlantic sector of the ACC one can expect a cumulative cooling effect and input of freshwater near oceanic fronts. The role of fronts has been only

briefly mentioned in the study on iceberg evolution by Rackow and others (2017), however, a detailed analysis is still missing. Finally, our study could shed light on the potential impacts on temperature, salinity and atmospheric CO₂ by the armada of icebergs released during Heinrich events or future disintegrations of ice shelves (Hellmer and others, 2012).

Supplementary material. The supplementary material for this article can be found at <https://doi.org/10.1017/jog.2025.10060>.

Acknowledgements. Thanks to Captain of RV *Polarstern* Stefan Schwarze and his crew. Thanks to the chief scientists Victor Smetacek and Syed Wajih A. Naqvi, to Denis Pierrot for revising the fCO₂ data. The speculation about the effect of disintegrating icebergs at glacial terminations started in a discussion with Howie Spero. Comments by two anonymous reviewers and by the editors Rachel Carr and Frank Pattyn helped us to improve the manuscript. This research was carried out under the CSIR-NIO, India supported projects NWP0014, OLP 2006, and OLP 2005. This is CSIR-NIO contribution no. 7426.

Author contributions. D.A.W.-G. wrote the first draft of the manuscript and performed most calculations, I.B. analyzed trajectories of large icebergs, G.S. measured carbonate system parameters, M.G.G. contributed chlorophyll data, M.V. measured hydrographic data, C.K. processed the pigment data, contributed the figures and improved the text and interpretation of the first draft. All authors discussed the results and contributed to the final version of the manuscript.

Competing interests. The authors have no competing interests.

References

- Babu GJ and Feigelson ED** (1992) Analytical and Monte Carlo comparisons of six different linear least squares fits. *Communications in Statistics - Simulation and Computation* **21**, 533–549.
- Budge JS and Long DG** (2018) A comprehensive database for Antarctic iceberg tracking using scatterometer data. *IEEE Journal of Selected Topics in Applied Earth Observations and Remote Sensing* **11**, 434–442.
- Davison BJ and 8 others** (2023) Annual mass budget of Antarctic ice shelves from 1997 to 2021. *Science Advances* **9**, eadi0186.
- Diemand D** (1984) Iceberg temperatures in the North Atlantic - theoretical and measured. *Cold Regions Science and Technology* **9**, 171–178.
- Draper NR and Smith H** (1998) *Applied Regression Analysis*, 3rd Edition, New York: John Wiley and Sons.
- Duprat LPAM, Bigg GR and Wilton DJ** (2016) Enhanced southern ocean marine productivity due to fertilization by giant icebergs. *Nature Geoscience* **9**, 219–221. doi:10.1038/NNGEO2633
- England MR, Wagner TJW and Eisenman I** (2020) Modeling the breakup of tabular icebergs. *Science Advances* **6**, eabd1273.
- Gade HG** (1979) Melting of ice in sea water: A primitive model with application to the Antarctic ice shelf and icebergs. *Journal of Physical Oceanography* **9**, 189–198.
- Gill AE** (1982) *Atmosphere-Ocean Dynamics (International Geophysics Series, Volume 30)*. Orlando: Academic Press. p. 662.
- Hardy A** (1967) *Great Waters - A Voyage of Natural History to Study Whales, Plankton and the Waters of the Southern Ocean in the Old Royal Research Ship Discovery With the Results Brought up to Date by the Findings of the R.R.S. Discovery II*, London: Collins. p. 542.
- Heinrich H** (1988) Origin and consequences of cyclic ice rafting in the Northeast Atlantic Ocean during the past 130,000 years. *Quaternary Research* **29**, 142–152.
- Hellmer HH, Kauker F, Timmermann R, Determann J and Rae J** (2012) Twenty-first-century warming of a large Antarctic ice-shelf cavity by a redirected coastal current. *Nature* **485**, 225–228. doi:10.1038/nature11064
- Helly JJ, Kaufmann RS, Stephenson Jr GR and Vernet M** (2011) Cooling, dilution and mixing of ocean water by free-drifting icebergs in the Weddell Sea. *Deep-Sea Research Part II: Topical Studies in Oceanography* **58**, 1346–1363. doi:10.1016/j.dsr2.2010.11.010
- Hemming SR** (2004) Heinrich events: Massive late Pleistocene detritus layers of the North Atlantic and their global climate imprint. *Reviews of Geophysics* **42**, RG1005. doi:10.1029/2003RG000128
- Henson** (2023) Coastal freshening drives acidification state in Greenland fjords. *Science of the Total Environment* **855**, 158962.
- Isobe T, Feigelson ED, Akritas MG and Babu GJ** (1990) Linear regression in astronomy. *The Astrophysical Journal* **364**, 104–113.
- Knap AH, Michaels A, Close AR, Ducklow H and Dickson AG** (1996) *Protocols for the joint global ocean flux study (JGOFS) core measurements. JGOFS, Reprint of the IOC Manuals and Guides No. 29, UNESCO 1994*, 19, Paris.
- Lee S-Y, Chiang JCH, Matsumoto K and Tokos KS** (2011) Southern Ocean wind response to North Atlantic cooling and the rise in atmospheric CO₂: Modeling perspective and paleoceanographic implications. *Paleoceanography* **26**, PA1214. doi:10.1029/2010PA002004
- Løset S** (1993) Numerical modelling of the temperature distribution in tabular icebergs. *Cold Regions Science and Technology* **21**, 103–115.
- Martin P and 14 others** (2013) Iron fertilization enhanced net community production but not downward particle flux during the Southern Ocean iron fertilization experiment LOHAFEX. *Global Biogeochemical Cycles* **27**, 871–881. doi:10.1002/gbc.20077
- Matthews JB and Quinlan AV** (1975) Seasonal characteristics of water masses in Muir Inlet, a fjord with tidewater glaciers. *Journal of the Fisheries Research Board of Canada* **32**, 1693–1703.
- Meire L and 8 others** (2015) Glacial meltwater and primary production are drivers of strong CO₂ uptake in fjord and coastal waters adjacent to the Greenland Ice Sheet. *Biogeosciences* **12**, 2347–2363.
- Merchant CJ and 15 others** (2019) Satellite-based time-series of sea-surface temperature since 1981 for climate applications. *Scientific Data* **6**(223), 1–18. doi:10.1038/s41597-019-0236-x
- Merino N and 6 others** (2016) Antarctic icebergs melt over the Southern Ocean: Climatology and impact on sea ice. *Ocean Model* **104**, 99–110. doi:10.1016/j.ocemod.2016.05.001
- Murty VSN and 9 others** (2010). Physical oceanography. In Smetacek V SWA Naqvi (ed.), *The expedition of the research vessel 'Polarstern' to the Antarctic in 2009 (ANT-XXV/3-LOHAFEX)*, 16–26, Alfred Wegener Institute for Polar and Marine Research, Berichte zur Polar-und Meeresforschung (Reports on Polar and Marine Research), volume 613.
- Nansen F** (1906) Northern Waters: Captain Roald Amundsen's Oceanographic Observations in the Arctic Seas in 1901: with a Discussion of the Origin of the Bottom-waters of the Northern Seas. *Videnskabs-Selskabets Skrifter. I. Mathematisk-Naturv. Klasse 1906 No. 3*, 145 pp.
- Nansen F** (1912) Das Bodenwasser und die Abkühlung des Meeres. *Internationale Revue der gesamten Hydrobiologie und Hydrographie* **5**, 1–42.
- Orsi AH, Whitworth T and Nowlin WD** (1995) On the meridional extent and fronts of the Antarctic Circumpolar Current. *Deep-Sea Research Part I: Oceanographic Research Papers* **42**, 641–673.
- Petrich C and Eicken H** (2010) *Growth, structure and properties of sea ice. Sea Ice - An Introduction to its Physics, Chemistry, Biology and Geology*, ed. In 2nd edition Thomas DN, and GS Dieckmann, Oxford, UK: Blackwell, pp.23–77.
- Petterson O** (1878) On the properties of water and ice. *Øfversigt af Kongl. Vetenskaps-akademiens förhandlingar* **2**, 61–78.
- Petterson O** (1900) Die Wasserzirkulation im Nordatlantischen Ozean. *Petermanns Geographische Mitteilungen* **7**, 61–65.
- Petterson O** (1904) On the influence of ice-melting upon oceanic circulation. *The Geographical Journal* **24**, 285–333.
- Petterson O** (1907) On the influence of ice-melting upon oceanic circulation. *The Geographical Journal* **30**, 273–295.
- Pratihary AK, Baraniya D and Naqvi SWA** (2010). Macro nutrients. In Smetacek V SWA Naqvi (ed.), *The expedition of the research vessel 'Polarstern' to the Antarctic in 2009 (ANT-XXV/3-LOHAFEX)*, 29–30, Alfred Wegener Institute for Polar and Marine Research, Berichte zur Polar-und Meeresforschung (Reports on Polar and Marine Research), volume 613.
- Rackow T, Wesche C, Timmermann R, Hellmer HH, Juricke S and Jung T** (2017) A simulation of small to giant Antarctic iceberg evolution: Differential impact on climatology estimates. *Journal of Geophysical Research-Oceans* **122**, 3170–3190. doi:10.1002/2016JC012513

- Raiswell R, Benning LG, Tranter M and Tulaczyk S** (2008) Bioavailable iron in the southern ocean: the significance of the iceberg conveyor belt. *Geochemical Transactions*, **9**, 9. doi:[10.1186/1467-4866-9-7](https://doi.org/10.1186/1467-4866-9-7)
- Roche D, Paillard D and Cortijo E** (2004) Constraints on the duration and freshwater release of Heinrich event 4 through isotope modelling. *Nature* **432**, 379–382. doi:[10.1038/nature03059](https://doi.org/10.1038/nature03059)
- Scambos T, Sergienko O, Sargent A, MacAyeal D and Fastook J** (2005) ICESat profiles of tabular iceberg margins and iceberg breakup at low latitudes. *Geophysical Research Letters* **32**, L23S09. doi:[10.1029/2005GL023802](https://doi.org/10.1029/2005GL023802)
- Schulz I and 10 others** (2018) Remarkable structural resistance of a nanoflagellate-dominated plankton community to iron fertilization during the Southern Ocean experiment LOHAFEX. *Marine Ecology Progress Series* **601**, 77–95. doi:[10.3354/meps12685](https://doi.org/10.3354/meps12685)
- Smetacek V and Naqvi SWA** (2010). The expedition of the research vessel 'Polarstern' to the Antarctic in 2009 (ANT-XXV/3-LOHAFEX). *Berichte zur Polar-und Meeresforschung (Reports on Polar and Marine Research)*, **613**.
- Smith RM and Bigg GR** (2023) Impact of giant iceberg A68A on the physical conditions of the surface South Atlantic, derived using remote sensing. *Geophysical Research Letters* **50**, e2023GL104028.
- Stephenson Jr GR, Sprintall J, Gille ST, Vernet M, Helly JJ and Kaufmann RS** (2011) Subsurface melting of a free-floating Antarctic iceberg. *Deep-Sea Research Part II-Topical Studies in Oceanography* **58**, 1336–1345.
- Straneo F and Cenedese C** (2015) The dynamics of Greenland's glacial fjords and their role in climate. *Annual Review of Marine Science* **7**, 89–112. doi:[10.1146/annurev-marine-010213-135133](https://doi.org/10.1146/annurev-marine-010213-135133)
- Tarling GA and 11 others** (2024) Collapse of a giant iceberg in a dynamic Southern Ocean marine ecosystem: in situ observations of A-68A at South Georgia. *Progress in Oceanography* **226**, 103297. doi:[10.1016/j.pocean.2024.103297](https://doi.org/10.1016/j.pocean.2024.103297)
- Vernet M, Sines K, Chakos D, Cefarelli AO and Ekern L** (2011) Impacts on phytoplankton dynamics by free-drifting icebergs in the NW Weddell Sea. *Deep-Sea Research Part II: Topical Studies in Oceanography* **58**, 1422–1435. doi:[10.1016/j.dsr2.2010.11.022](https://doi.org/10.1016/j.dsr2.2010.11.022)
- Weiss RF** (1974) Carbon dioxide in water and seawater: the solubility of a non-ideal gas. *Marine Chemistry* **2**, 203–215.
- Zeebe RE and Wolf-Gladrow D** (2001) *CO₂ in Seawater: Equilibrium, Kinetics, Isotopes: Equilibrium, Kinetics, Isotopes*. Amsterdam: Elsevier, p. 346.